

## The Aharonov-Bohm wave and the Cornu spiral

This article has been downloaded from IOPscience. Please scroll down to see the full text article.

1999 J. Phys. A: Math. Gen. 32 L447

(<http://iopscience.iop.org/0305-4470/32/42/101>)

View [the table of contents for this issue](#), or go to the [journal homepage](#) for more

Download details:

IP Address: 171.66.16.111

The article was downloaded on 02/06/2010 at 07:47

Please note that [terms and conditions apply](#).

## LETTER TO THE EDITOR

**The Aharonov–Bohm wave and the Cornu spiral**M V Berry<sup>†</sup> and A Shelankov<sup>‡</sup><sup>†</sup> H H Wills Physics Laboratory, Tyndall Avenue, Bristol BS8 1TL, UK<sup>‡</sup> Department of Physics, University of Umeå, SE-901 87 Umeå, Sweden

Received 8 July 1999

**Abstract.** For flux  $\alpha$ , the Aharonov–Bohm wavefunction  $\Psi_{AB}(r, \alpha)$  is represented exactly in terms of Fresnel integrals. Numerical evidence shows that in the complex  $\Psi_{AB}$  plane the wave clings to the Cornu spiral for all positions  $r$  except very close to the flux line, that is, the argument  $w(r, \alpha)$  of the Fresnel integrals is almost real. This is confirmed by deriving an asymptotic expansion for  $w$  in powers of  $1/r$ .

Our purpose is to describe and explain a remarkable property of the Aharonov–Bohm (AB) wave  $\Psi_{AB}(r, \alpha)$  (Aharonov and Bohm 1959, Olariu *et al* 1985), describing the scattering of a plane wave of quantum particles with charge  $q$  by a magnetic field confined to a line with (quantum) flux  $\alpha$ , that is, by the inaccessible field

$$\mathbf{B}(r) = \nabla \times \mathbf{A}(r) = \frac{h}{q} \alpha \delta(r). \quad (1)$$

The property is that  $\Psi_{AB}$  has a natural and convenient geometrical representation in terms of the Cornu spiral (Fresnel integral) of optics. This was discovered through numerical explorations, motivated by the fact that  $\Psi_{AB}$  is given by a Fresnel integral exactly for  $\alpha = \frac{1}{2}$  (Aharonov and Bohm 1959), and in the paraxial approximation (that is, near the forward direction) for all  $\alpha$ .

In the  $r$  plane we use coordinates  $r = (x, y) = (r \cos \theta, r \sin \theta)$ , and consider the incident plane wave travelling in the positive  $x$  direction. We choose the wavenumber  $k = 1$  (equivalent to measuring distances in units of wavelength/ $(2\pi)$ ).

We begin with the paraxial approximation (Shelankov 1998, Berry 1999), which is most easily implemented in the sheet gauge where, with  $\Theta$  denoting the unit step

$$\mathbf{A}(r) = \mathbf{A}_s(r) = -\frac{\alpha}{2} \delta(x) [\Theta(y) - \Theta(-y)] e_x. \quad (2)$$

In this approximation, back-scattered waves are neglected, and  $\mathbf{A}_s$  acts like a phase-changing screen at  $x = 0$ , generating the near-forward wave

$$\begin{aligned} \Psi_{AB}(r) &\approx \Psi_{AB, \text{paraxial}}(r) \\ &= \frac{\exp\{i(x - \frac{1}{4}\pi)\}}{\sqrt{2\pi x}} \int_{-\infty}^{\infty} dy' \exp\left\{i\left[-\pi\alpha \text{sgn}y' + \frac{(y - y')^2}{2x}\right]\right\} \\ &= \exp(ix) \left[ \cos(\pi\alpha) - \sin(\pi\alpha) \exp\left(\frac{1}{4}i\pi\right) \sqrt{2} F\left(\frac{y}{\sqrt{x}}\right) \right]. \quad (3) \end{aligned}$$

Here  $F$  denotes the Fresnel integral, which we here define as

$$F(w) \equiv \int_0^{w/\sqrt{\pi}} dt \exp(\frac{1}{2}i\pi t^2). \tag{4}$$

As  $w$  varies from  $-\infty$  to  $+\infty$  through real values, the parametric plot of  $F(w)$  in the complex  $F$  plane describes the Cornu spiral (Born and Wolf 1959).

Motivated by the form of (3), and now reverting to the more familiar circular gauge

$$A(r) = A_c(r) \equiv \frac{h}{q} \frac{\alpha}{2\pi r} e_\theta \tag{5}$$

we define the *cornuified wave*  $K$  for the exact AB wave by

$$\Psi_{AB}(r) = \exp[i(x + \alpha\theta)] [\cos(\pi\alpha) - \sin(\pi\alpha) \exp(\frac{1}{4}i\pi) \sqrt{2}K(r, \alpha)] \tag{6}$$

that is

$$K(r, \alpha) \equiv \frac{\exp(-\frac{1}{4}i\pi)}{\sqrt{2} \sin(\pi\alpha)} [\cos(\pi\alpha) - \exp(-i(x + \alpha\theta)) \Psi_{AB}(r, \alpha)]. \tag{7}$$

Now we can define our main object of study: the function  $w(r, \alpha)$  defined implicitly and uniquely by

$$K(r, \alpha) \equiv F(w(r, \alpha)) = \int_0^{w(r, \alpha)/\sqrt{\pi}} dt \exp(\frac{1}{2}i\pi t^2). \tag{8}$$

When  $w$  is real, the cornuified wave lies on the Cornu spiral in the complex  $K$  plane. This is the case paraxially, as in (3), where  $w = y/\sqrt{x}$ , and for  $\alpha = \frac{1}{2}$ , where (Aharonov and Bohm 1959)  $w = \sqrt{[2(r - x)]} = 2 \sin(\theta/2)\sqrt{r}$ . Non-zero imaginary parts of  $w$  will correspond to points off the spiral.

It is easy to compute  $K$  numerically via the representation of  $\Psi_{AB}$  in the circular gauge (Aharonov and Bohm 1959) as a convergent series of Bessel functions (with  $\theta$  replaced by  $\theta + \pi$  because the original AB wave travelled in the direction  $-x$  rather than  $+x$ )

$$\Psi_{AB}(r, \alpha) = \sum_{m=-\infty}^{\infty} (-i)^{|m-\alpha|} \exp\{im(\theta + \pi)\} J_{|m-\alpha|}(r). \tag{9}$$

Figure 1 shows how  $K$  condenses onto the Cornu spiral as  $r$  increases. This is the phenomenon we wish to explain. Even when  $r = 1$ , that is  $1/(2\pi)$  wavelengths from the flux line, the wave follows the spiral rather closely. As  $r$  increases, the cornuified wave explores more of the spiral, as expected from the solution for  $\alpha = \frac{1}{2}$  with the extreme values (in the backward direction  $\theta = \pm\pi$ )  $w = \pm 2\sqrt{r}$ , corresponding to the two ‘eyes’ of the spiral (the origin corresponds to the forward direction  $\theta = 0$ ). As is evident from the groups of points with different  $\alpha$ , the Fresnel argument  $w(r, \alpha)$  depends on flux, as we will soon explore in detail.

$\Psi_{AB}$  is a single-valued function of position but  $K$  is not; (6) or (7) imply the following continuation rule in the backward direction  $\theta = \pm\pi$ :

$$\exp(i\pi\alpha)K(\pi, r, \alpha) - \exp(-i\pi\alpha)K(-\pi, r, \alpha) = (1 + i) \cos \pi\alpha. \tag{10}$$

Moreover,  $\Psi_{AB}$  vanishes at the origin, but  $K$  takes the value

$$K(r, \alpha) \rightarrow \frac{\cot(\pi\alpha)}{1 + i} \quad \text{as } r \rightarrow 0. \tag{11}$$

Therefore the backward discontinuity (10) must disappear as  $r \rightarrow 0$ , and indeed the value (11) is the condition for this. This limit represents an extreme departure from the spiral of figure 1,

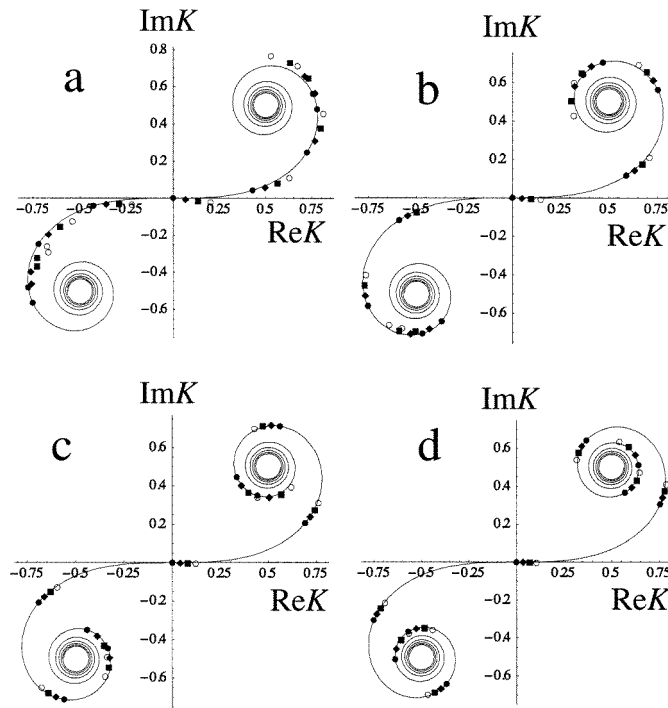


**Figure 1.** Cornuified AB wave  $K(r, \alpha)$  (equation (7)), for  $\alpha = \frac{1}{8}$  (open circles),  $\alpha = \frac{1}{4}$  (squares),  $\alpha = \frac{3}{8}$  (diamonds),  $\alpha = \frac{1}{2}$  (filled circles) and  $\theta = \{-\pi, -3\pi/4, -\pi/2, -\pi/4, 0, \pi/4, \pi/2, 3\pi/4, \pi\}$ , compared with the Cornu spiral (full curve); (a):  $r = 1$ , (b):  $r = 2$ , (c):  $r = 3$ , (d):  $r = 4$ .

with points representing  $K$  condensing onto the line with slope  $-\pi/4$ , anchored at the origin  $K = 0$  for  $\alpha = \frac{1}{2}$ , the values of  $K$  depending only on  $\alpha$  and not on  $\theta$ .

The AB wave (9) has the following symmetries:

$$\begin{aligned} \Psi_{AB}(r, \alpha + 1) &= -\exp(i\theta)\Psi_{AB}(r, \alpha) \\ \Psi_{AB}(r, \theta, -\alpha) &= \Psi_{AB}(r, -\theta, \alpha) \end{aligned} \tag{12}$$

enabling us to restrict the range of  $\alpha$  to  $0 \leq \alpha \leq \frac{1}{2}$ —although all subsequent formulae will be valid in the larger interval  $0 \leq \alpha < 1$ . Moreover, although  $\Psi_{AB}$  is a periodic function of  $\theta$  we will find it convenient to restrict angles to the range  $-\pi \leq \theta \leq \pi$ , and confirm later that the wave is single-valued according to (10).

To manipulate  $\Psi_{AB}$  into the form (6), we first note that recurrence formulae for Bessel functions enable the radial and angular derivatives to be written (generalizing an equation in Aharonov and Bohm (1959)) as (denoting derivatives  $\partial/\partial x$  by  $\partial_x$ )

$$\begin{aligned} \left( \frac{\partial_r}{\frac{1}{r}\partial_\theta} \right) \exp\{-i(r \cos \theta + \alpha\theta)\}\Psi_{AB}(r, \alpha) &= \frac{1}{2} \sin(\pi\alpha) \exp\{-i(r \cos \theta + \alpha\theta)\} \\ &\times \left[ iH_{1-\alpha}^{(1)}(r) \exp\left(-\frac{1}{2}i\pi\alpha\right) \begin{pmatrix} -1 \\ +1 \end{pmatrix} H_\alpha^{(1)}(r) \exp\left(i\left(\frac{1}{2}\pi\alpha + \theta\right)\right) \right]. \end{aligned} \tag{13}$$

(It is interesting to note that these equations imply a relation between the two first derivatives

of  $\Psi_{AB}$  and its mixed second derivative.) Now, integrating the radial derivative,

$$\Psi_{AB}(\mathbf{r}, \alpha) = \frac{1}{2} \sin(\pi\alpha) \exp(ix) \int_0^r d\rho \exp(-i\rho \cos \theta) \times [iH_{1-\alpha}^{(1)}(\rho) \exp(-\frac{1}{2}i\pi\alpha) - H_{\alpha}^{(1)}(\rho) \exp(i(\frac{1}{2}\pi\alpha + \theta))]. \quad (14)$$

Next, we change the integration range using (Gradshteyn and Ryzhik 1980)

$$\int_0^{\infty} d\rho H_{\alpha}^{(1)}(\rho) \exp(-i\rho \cos \theta) = 2 \exp\left(-\frac{1}{2}i\pi\alpha\right) \frac{\sin(\pi \operatorname{sgn}\theta - \theta)}{\sin \theta \sin(\pi\alpha)} \quad (|\theta| \leq \pi). \quad (15)$$

Thus

$$\Psi_{AB}(\mathbf{r}, \alpha) = \exp\{i(x + \alpha(\theta - \pi \operatorname{sgn}\theta))\} - \frac{1}{2} \sin(\pi\alpha) \exp(ix) \int_r^{\infty} d\rho \exp(-i\rho \cos \theta) \times [iH_{1-\alpha}^{(1)}(\rho) \exp(-\frac{1}{2}i\pi\alpha) - H_{\alpha}^{(1)}(\rho) \exp(i(\frac{1}{2}\pi\alpha + \theta))]. \quad (16)$$

Despite appearances, this function is smooth near the forward direction  $\theta = 0$ . It is well known that away from the forward direction the first term represents the incident plane wave, and the second term the scattered wave (decaying as  $1/\sqrt{r}$  for large  $r$ ) (Aharonov and Bohm 1959, Berry *et al* 1980, Olariu *et al* 1985).

To transform the awkward representation (16) into the more transparent form given by (4), (6) and (8), we note that

$$\cos(\pi\alpha) - \sin(\pi\alpha) \exp(\frac{1}{4}i\pi) \sqrt{2} \int_0^{w/\sqrt{\pi}} dt \exp(\frac{1}{2}i\pi t^2) = \exp(-i\pi\alpha \operatorname{sgn}\theta) + \sin(\pi\alpha) \exp(\frac{1}{4}i\pi) \sqrt{2} \int_{w/\sqrt{\pi}}^{\infty \operatorname{sgn}\theta} dt \exp(\frac{1}{2}i\pi t^2) \quad (17)$$

and that the leading-order large- $\rho$  asymptotics of the Bessel functions in (14) (Abramowitz and Stegun 1972) imply

$$iH_{1-\alpha}^{(1)}(\rho) \exp(-\frac{1}{2}i\pi\alpha) - H_{\alpha}^{(1)}(\rho) \exp(i(\frac{1}{2}\pi\alpha + \theta)) \approx -2\sqrt{\frac{2}{\pi\rho}} \sin(\frac{1}{2}\theta) \times \exp\{i(\rho + \frac{1}{2}\theta + \frac{1}{4}\pi)\}. \quad (18)$$

Then, after a little reduction, including transforming the integration variable in (16) from  $\rho$  to  $t = 2 \sin(\theta/2)\sqrt{(\rho/\pi)}$ , we obtain the equation satisfied by the leading-order approximation to  $w(\mathbf{r}, \alpha)$ :

$$\int_{w/\sqrt{\pi}}^{\infty \operatorname{sgn}\theta} dt \exp(\frac{1}{2}i\pi t^2) \approx \exp\{i\theta(\frac{1}{2} - \alpha)\} \int_{2 \sin(\frac{1}{2}\theta)\sqrt{r/\pi}}^{\infty \operatorname{sgn}\theta} dt \exp(\frac{1}{2}i\pi t^2). \quad (19)$$

Differentiation with respect to  $r$  now leads to the identification

$$w(\mathbf{r}, \alpha)^2 \rightarrow w_0(\mathbf{r}, \alpha)^2 \equiv 4r \sin^2(\frac{1}{2}\theta) + 2\theta(\frac{1}{2} - \alpha) \quad \text{as } r \rightarrow \infty. \quad (20)$$

(This procedure should be distinguished from the superficially similar argument leading to equation (2.12) of Olariu *et al* (1985) that also involves a Fresnel integral, obtained by substituting (18) into (16) directly and evaluating the  $\rho$  integral; by contrast, our Cornu representation is manifestly smooth near the forward direction.)

To get corrections to  $w$ , we replace (18) by the formally exact asymptotic Hankel expansion (Gradshteyn and Ryzhik 1980), combine (16) and (17), and differentiate with respect to  $r$ . This gives, after some reduction, the following differential equation:

$$\exp\{\frac{1}{2}i(w^2 - w_0^2)\} \sqrt{r} \partial_r w = [1 + (i(\frac{1}{2} - \alpha) + 2r \partial_r^2) Q] \sin(\frac{1}{2}\theta) \quad (21a)$$

where

$$Q = \frac{\cos \pi \alpha}{2\pi r} \sum_{m=0}^{\infty} \frac{(m - \frac{1}{2} + \alpha)!(m + \frac{1}{2} - \alpha)!}{(2ir)^m (m + 1)!}. \quad (21b)$$

Next, we write  $w$  as

$$w(r, \alpha)^2 = w_0^2(r, \alpha) + v(r, \alpha). \quad (22)$$

Then  $v(r, \alpha)$  is determined by

$$\exp\left(\frac{1}{2}iv\right) \frac{\left(1 + \frac{\partial_r v}{4 \sin^2(\frac{1}{2}\theta)}\right)}{\sqrt{1 + \frac{2\theta(\frac{1}{2}-\alpha)+v}{4r \sin^2(\frac{1}{2}\theta)}}} = 1 + \frac{1}{\sin(\frac{1}{2}\theta)} \left[ \left(i\left(\frac{1}{2} - \alpha\right) + 2r\partial_{r\theta}^2\right) \right] Q \sin\left(\frac{1}{2}\theta\right). \quad (23)$$

To solve this, we express  $v$  as a power series in  $1/r$ , that is

$$v(r, \alpha) = \sum_{m=0}^{\infty} \frac{v_m(\theta, \alpha)}{r^m} \quad (v_0 = 1) \quad (24)$$

and identify the two sides term by term. This is a purely algebraic operation: no integrations are required in the solution, because the terms generated by  $\partial_r v$  depend on coefficients already found. In writing the results, it is convenient to define

$$\beta \equiv \frac{1}{2} - \alpha. \quad (25)$$

The first few coefficients (determined using Mathematica™ (Wolfram 1996) are

$$\begin{aligned} v_1(\theta, \alpha) &= -i \frac{\beta}{2 \sin^2(\frac{1}{2}\theta)} (\theta - \sin \theta) + \beta^2 \\ v_2(\theta, \alpha) &= \frac{1}{16 \sin^4(\frac{1}{2}\theta)} [\beta(8 \sin \theta - \sin 2\theta - 6\theta) - i\beta^2(7 - 2\theta^2 - 8 \cos \theta + \cos 2\theta)] \\ v_3(\theta, \alpha) &= \frac{1}{\sin^6(\frac{1}{2}\theta)} \left[ \frac{i\beta}{64} (30\theta - 45 \sin \theta + 9 \sin 2\theta - \sin 3\theta) \right. \\ &\quad \left. + \frac{\beta^2}{384} (84\theta^2 - 24\theta \sin \theta + 267 \cos \theta - 48 \cos 2\theta + 5 \cos 3\theta - 224) \right. \\ &\quad \left. - \frac{i\beta^3}{192} (8\theta^3 + 12\theta \cos \theta - 12\theta - 9 \sin \theta + 6 \sin 2\theta - \sin 3\theta) \right] + \frac{\beta^4}{12}. \end{aligned} \quad (26)$$

We have confirmed that with these coefficients the continuation rule (10) for the backward direction is satisfied order by order in  $1/r$ .

In the forward direction, all these coefficients are finite, notwithstanding the inverse powers of  $\sin(\theta/2)$ . The coefficients can be found as the limits of  $v_n(\theta, \alpha)$  as  $\theta \rightarrow 0$ . More conveniently, they can also be determined directly from the limiting form of (23) for small  $\theta$ . After a little reduction, this takes the form

$$\frac{\exp(\frac{1}{2}iv)r^2\partial_r v}{\sqrt{rv}} = -\frac{\sin \pi \beta}{\pi} \sum_{m=0}^{\infty} \left(\frac{-i}{2r}\right)^m \frac{(m + \beta)!(m - \beta)!}{m!} = 2r^2\partial_r Q \quad (27)$$

whence the lowest coefficient  $v_1(0, \alpha)$  is  $(\frac{1}{2} - \alpha)^2 = \beta^2$  and the rest follow by recursion. Defining

$$v_n(0, \alpha) = i^{n+1}u_n \quad (28)$$

we find

$$\begin{aligned}
 u_1 &= -\beta^2 & u_2 &= \frac{\beta^2}{3} \\
 u_3 &= \frac{\beta^4}{12} - \frac{41\beta^2}{180} & u_4 &= -\frac{8\beta^4}{45} + \frac{26\beta^2}{105} \\
 u_5 &= -\frac{\beta^6}{40} + \frac{835\beta^4}{2268} - \frac{199\beta^2}{525} \\
 u_6 &= \frac{2809\beta^6}{22\,680} - \frac{293\,761\beta^4}{340\,200} + \frac{10\,517\beta^2}{13\,860} \\
 u_7 &= \frac{5\beta^8}{448} - \frac{20\,681\beta^6}{42\,525} + \frac{23\,489\,777\beta^4}{9979\,200} - \frac{3177\,061\beta^2}{1681\,680} \\
 u_8 &= -\frac{21\,731\beta^8}{226\,800} + \frac{8502\,199\beta^6}{4490\,640} - \frac{1406\,426\,953\beta^4}{189\,189\,000} + \frac{5648\beta^2}{1001}.
 \end{aligned} \tag{29}$$

For general  $r$ , departures from the Cornu spiral (figure 1) are revealed in the imaginary part of  $v(r, \alpha)$  in (22). From the coefficients (26), it is clear that the deviations from the spiral are of order  $1/r$ , except in the forward direction when, as (28) and (29) show, the deviation is of order  $1/r^2$ .

Deviation from the spiral is measured by  $\text{Im } w$ . Another measure can be defined in terms of the rephased AB wave

$$\tilde{\Psi}_{AB} \equiv \exp\{-i(x + \alpha\theta)\}\Psi_{AB}. \tag{30}$$

The new measure (a kind of vorticity) is

$$\begin{aligned}
 \Gamma(r, \alpha) &= \text{Im } \nabla \tilde{\Psi}_{AB}^*(r) \times \nabla \tilde{\Psi}_{AB}(r) = \nabla \times \text{Im} [\tilde{\Psi}_{AB}^*(r) \nabla \tilde{\Psi}_{AB}(r)] \\
 &= \frac{\sin^2(\pi\alpha)}{2\pi|w|^2} \exp\{-2\text{Im}(w^2)\} \nabla[\text{Re}(w^2)] \times \nabla[\text{Im}(w^2)].
 \end{aligned} \tag{31}$$

Evidently,  $\Gamma$  vanishes if  $w$  is real, that is if the cornuified wave lies exactly on the spiral. An equivalent formula, that follows from (9) together with (13), is (for  $0 \leq \alpha < 1$ )

$$\Gamma(r, \alpha) = \frac{1}{4} \sin^2(\pi\alpha) [|H_{1-\alpha}^{(1)}(r)|^2 - |H_{\alpha}^{(1)}(r)|^2]. \tag{32}$$

From this formula, or from (30) with (22) and (26), follows the asymptotic relation

$$\Gamma(r, \alpha) \rightarrow \frac{(\frac{1}{2} - \alpha)}{2\pi r^3} \sin^2(\pi\alpha) \quad \text{as } r \rightarrow \infty \tag{33}$$

giving further evidence of how closely  $K$  clings to the spiral when  $r$  is not small.

The series (24), whose first few coefficients are given by (26) and (29), is divergent but enables  $w$ , and hence  $\Psi_{AB}$ , to be calculated with very high accuracy. To justify these assertions, we must first determine the high-order terms of the series. For economy of writing, we consider only the forward direction.

For  $n \gg 1$ , the coefficients  $u_n$  (defined by (28)) can be estimated by approximating the rhs of the governing equation (27) using Stirling's formula and noting that the dominant contributions from the lhs come from the term  $\partial_r v$  (because in this term—unlike the terms  $v$  in the exponential and denominator—the high orders in the series (24) are multiplied by  $m$ ). The result is the following 'asymptotics of the asymptics':

$$u_n \approx \beta \sin \pi\beta \frac{(-1)^n (n-2)!}{2^{n-1}\pi} \quad (n \gg 1). \tag{34}$$

Figure 2 shows how accurately this approximation captures the behaviour of the exact coefficients (29), even for quite small  $n$ .

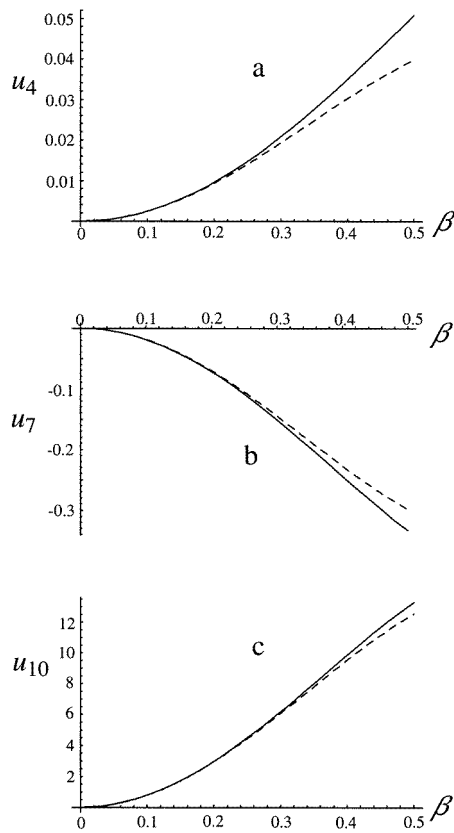


**Figure 2.** Full curves: coefficients  $u_n$  (from (28) and (29)) of the series (24) for points in the forward direction, as functions of flux  $\beta = \frac{1}{2} - \alpha$ , for the Fresnel argument (22); dashed curves: the approximation (34); (a)  $m = 4$ ; (b)  $m = 7$ ; (c)  $m = 10$ .

Thus the series (24) diverges factorially, in the manner familiar in asymptotic expansions (Dingle 1973), with terms initially decreasing when  $r$  is large. From Stirling's formula, the smallest term is near

$$m^* = \text{int}(2r + 1) \tag{35}$$

and its size is

$$\frac{|v_{m^*}|}{r^{m^*}} \approx \frac{\beta \sin \pi \beta}{\sqrt{\pi} r^{3/2}} \exp(-2r). \tag{36}$$

Asymptotics folklore suggests that the error in truncating the series (24) is of the same order as the first omitted term, so that the best approximation results from truncation at the least term. A more precise result can be derived by Borel summation (Dingle 1973, Berry 1989) of the tail of the series, using the approximation (34) and the fact that the phases of successive terms differ by  $\pi/2$ . The result is that if the truncation error is defined as

$$\text{error}(n) \equiv \left| v(r, \theta = 0, \alpha) - i \sum_{m=1}^n \frac{i^m u_m}{r^m} \right| \tag{37}$$

the error made by optimal truncation is  $1/\sqrt{2}$  times the least term (36). Thus

$$\text{error}(m^*) \approx \frac{|v_{m^*}|}{\sqrt{2} r^{m^*}} \approx \frac{\beta \sin \pi \beta}{\sqrt{2\pi} r^{3/2}} \exp(-2r). \tag{38}$$

Testing this estimate requires computation of  $v(r, \theta = 0, \alpha)$ , related to the Fresnel argument  $w$  by (22). To find  $v$ , we first computed the cornuified wave (7) from the AB



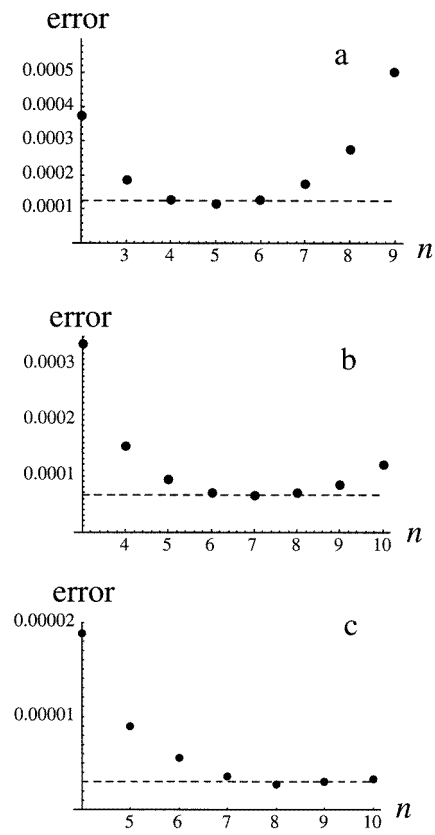


**Figure 3.** Dots: truncation error (37) in the series (24) for the Fresnel argument (22), for points  $r$  in the forward direction, with (a)  $r = 2, \alpha = \frac{3}{8}$ ; (b)  $r = 3, \alpha = \frac{1}{8}$ ; (c)  $r = 4, \alpha = \frac{1}{4}$ . Dashed line: the estimate (38).

series (9), equated this with the Fresnel integral (4) via (8), and then solved numerically for the argument  $w$ . As figure 3 shows, the error (37) thus calculated is remarkably close to the estimate (38).

With systematic improvement of the ‘asymptotics of the asymptotics’ (34), based on a more careful analysis of the governing equation (27), it should be possible to reduce the error (38) by further exponential factors using hyperasymptotic resummations (Berry and Howls 1991, Berry 1992), but we do not pursue this here.

Finally, we speculate on the physical reason why the AB wave is so intimately linked to the Cornu spiral, as we have demonstrated. In optics, the spiral appears in edge diffraction (Born and Wolf 1959), both in the original approximate theory of Fresnel and in the exact solution (Sommerfeld 1950) for diffraction by an impenetrable half-plane. In the sheet gauge (2), the vector potential acts as a phase-changing screen with a discontinuity—an edge, indeed, situated at the flux line  $x = y = 0$ .

But there are differences: in Sommerfeld’s wave, there are two Fresnel integrals, associated with the incident and reflected beams, unlike the AB screen which is transparent and where there is therefore only one Fresnel integral associated with the edge. This Cheshire-cat situation—an edge without an associated reflecting screen—is characteristic of the AB wave, where the edge is defined as a line around which the phase of the AB wave (after the vector potential has been gauged away) changes by  $2\pi\alpha$ . Perhaps the deviation of the argument  $w$  from the simple geometrical expression  $2(r - x)$  is determined by multiple windings about the edge, in a manner related to the whirling-wave representation of  $\Psi_{AB}$  (Berry 1980, Morandi and Menossi

1984, Rammer and Shelankov 1987); then the small exponential (36) might be interpreted, as is common in asymptotics, as an instanton in some complexified dynamics associated with the AB effect.

This work began at the Weizmann Institute (Rehovot, Israel) for whose hospitality we are grateful. AS thanks Michael Stone for numerical assistance in the early stages of this work, and the Swedish Natural Science Research Council for financial support.

## References

- Abramowitz M and Stegun I A 1972 *Handbook of Mathematical Functions* (Washington, DC: National Bureau of Standards)
- Aharonov Y and Bohm D 1959 Significance of electromagnetic potentials in the quantum theory *Phys. Rev.* **115** 485–91
- Berry M V 1980 Exact Aharonov–Bohm wavefunction obtained by applying Dirac’s magnetic phase factor *Eur. J. Phys.* **1** 240–4
- 1989 Uniform asymptotic smoothing of Stoke’s discontinuities *Proc. R. Soc. A* **422** 7–21
- 1992 *Asymptotics Beyond All Orders* ed H Segur and S Tanveer (New York: Plenum) pp 1–14
- 1999 Aharonov–Bohm beam deflection: Shelankov’s formula, exact solution, asymptotics and an optical analogue *J. Phys. A: Math. Gen.* **32** 5627–41
- Berry M V, Chambers R G, Large M D, Upstill C and Walmsley J C 1980 Wavefront dislocations in the Aharonov–Bohm effect and its water-wave analogue *Eur. J. Phys.* **1** 154–62
- Berry M V and Howls C J 1991 Hyperasymptotics for integrals with saddles *Proc. R. Soc. A* **434** 657–75
- Born M and Wolf E 1959 *Principles of Optics* (London: Pergamon)
- Dingle R B 1973 *Asymptotic Expansions: their Derivation and Interpretation* (New York: Academic)
- Gradshteyn I S and Ryzhik I M 1980 *Tables of Integrals, Series and Products* (New York: Academic)
- Morandi G and Menossi E 1984 Path-integrals in multiply-connected spaces and the Aharonov–Bohm effect *Eur. J. Phys.* **5** 49–58
- Olariu S and Popescu I I 1985 The quantum effects of electromagnetic fluxes *Rev. Mod. Phys.* **57** 339–436
- Rammer J and Shelankov A 1987 Weak localization in inhomogeneous magnetic fields *Phys. Rev. B* **36** 3135–46
- Shelankov A 1998 Magnetic force exerted by the Aharonov–Bohm flux line *Europhys. Lett.* **43** 623–8
- Sommerfeld A 1950 *Optics: Lectures on Theoretical Physics* vol 4 (New York: Academic)
- Wolfram S 1996 *The Mathematica Book* (Cambridge: Cambridge University Press)